26th IMEKO TC4 International Symposium
24th International Workshop on ADC and DAC Modelling and Testing
IMEKO TC-4 2023
Pordenone, Italy / September 20-21, 2023

First results on torque estimation by FEA and experimental analysis in a novel CSFH-based microgripper

Gabriele Bocchetta[1], Giorgia Fiori[1], Federico Filippi[1], Pietro Ursi[2], Salvatore Andrea Sciuto[1], Andrea Scorza[1]

[1] *Dep. of Industrial, Electronic and Mechanical Engineering, Roma TRE University, Rome, Italy*
[2] *Dep. of General Surgery and Surgical Specialties "Paride Stefanini", Sapienza University of Rome, Rome, Italy*

***Abstract* – Microgrippers (MGs) are MEMS devices that can manipulate cells and microscopic objects. In this work an approach based on both experimental and a finite element analysis is proposed with the aim of evaluating the torque exerted by the micro-actuator of a novel prototype of MG equipped with electrostatic rotary comb-drives and Conjugate Surface Flexure Hinges (CSFHs) when powered by a 0-20 V peak-to-peak supply voltage. The angular displacement of the micro-actuator has been measured using an image analysis method implemented by the Authors from videos acquired by a camera on a trinocular optical microscope, while the hinge stiffness has been estimated using numerical simulations: the obtained results show that the comb-drive can apply a maximum torque of 1.4 ± 0.2 nNm.**

I. INTRODUCTION

Nowadays, the development of MEMS (Micro Electro-Mechanical Systems) devices is becoming increasingly widespread. Microgrippers (MGs) are devices that have been extensively investigated during the last two decades as potential tools for a wide range of possible applications [1-3], especially in the biomedical field [4-5]. Microgrippers' versatility has lately been demonstrated in operations such as versatile grasping and autonomous pick-and-place [6-7]. MG prototypes embedded with Conjugate Surface Flexure Hinges (CSFHs) [8,9] performed successfully in grasping and releasing agarose microspheres in waterdrops [10]. The CSFH is depicted in detail in Fig. 1. Recent studies have shown that the total number of CSFHs is proportional to the energy necessary to deform the MG structure. As a result, MGs with only one CSFH pair and one pair of electrostatic rotary-comb drives [11-12] demonstrated a wider range of displacement considering the same applied voltage than MGs composed of a double four-bar linkage with multiple CSFHs [13-14].

The present work focuses for the first time on a novel CSFH-based MG equipped with only one CSFH pair, with the aim of investigating the mechanical behavior of the

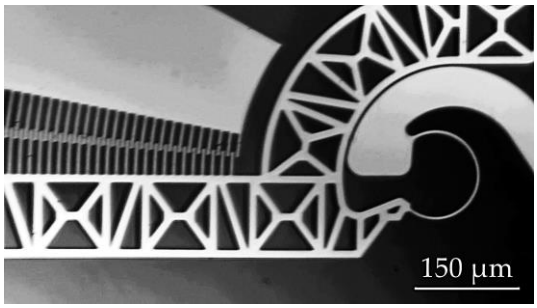

Fig. 1. CSFH and portion of the electrostatic comb-drive.

hinges by means of experimental analysis, based on image analysis method [15], and Finite Element Analysis (FEA), evaluating the torque exerted by electrostatic micro-actuators. A supply voltage in the 0-20 V range has been considered for the Device Under Test (DUT), whose main parameters are listed in Table 1. Since the DUT is free to move, i.e., it does not carry out a manipulation operation, each position assumed during movement has been assessed as an equilibrium condition between the torque exerted by the electrostatic actuator and the resistant torque due to the elastic behavior of the CSFH, which allows the actuation torque estimation as:

$$\tau = k\vartheta \tag{1}$$

where τ stands for the comb-drive's torque, while k and ϑ indicate the CSFH stiffness coefficient and the micro-actuator's angular displacement, respectively. As a first approximation, by considering CSFHs homogeneous, linear elastic beams with uniform, rectangular cross sections and assuming the bending moment as constant, it is possible to estimate the stiffness coefficient k [16-17]:

$$k \cong \frac{1}{12}\frac{Ebh^3}{r_n\alpha} \tag{2}$$

where E indicates the Young's modulus, b is the device thickness, h is the curved beam width, r_n is the neutral axis curvature radius, and α is the subtended angle by the latter. In particular, the experimental analysis aims to measure

Table 1. Microgripper main specifications

Component		Symbol	Value
SOI Wafer	Device layer thickness	b	40 μm
CSFH	Curved beam width	h	5 μm
	Neutral axis curvature radius	r_n	62.5 μm
	Curved beam subtended angle	α	240.9°
Fingers	Number per comb-drive	n	64
	Width	d	4 μm
	Rotor-stator distance	g	3 μm

the actual angular displacement of the micro-actuator, while through FEA the stiffness coefficient of the curved beam can be estimated.

II. MATERIALS AND METHODS

The DUT shown in the 3D rendering in Fig. 2 is a newly developed MG prototype fabricated monolithically by the DRIE (Deep Reactive Ion Etching) process on a SOI (Silicon-on-Insulator) wafer with an aluminum hard mask [18]. Several experimental tests have been carried out to measure the comb-drive angular displacement. In particular, many videos have been recorded using a trinocular optical microscope equipped with a video camera at different magnification levels to capture video of the entire micro-actuator and the CSFH. The acquired videos have been analyzed through a measurement procedure developed in MATLAB. Finally, in order to evaluate the stiffness coefficient, a finite element model (in COMSOL Multiphysics environment), has been implemented by numerically simulating the angular displacement of the micro-actuator as a function of electric potential. The numerical simulations that have been carried out, have as a base the results obtained during the experimental phase. In this way it has been possible to evaluate the stiffeness of the CSFH considering the same comb-drive rotation and the supply voltage used for the actuation of the DUT.

A. Experimental Analysis

The experimental setup implemented to conduct the experimental testing on the DUT consists of the power supply instrumentation, which includes a function generator, a power amplifier, and micropositioners for positioning tungsten needles that power the MG via contact, as well as the image acquisition instrumentation [19], including a trinocular optical microscope with a video camera. The specifications of the main components are listed in Table 2.

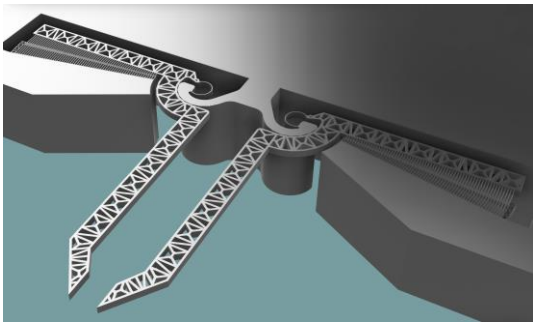

Fig. 2. 3D rendering of the microgripper prototype.

Table 2. Experimental setup main components

Device	Characteristics
Function Generator	Amplitude: 0 to ± 10 V peak-to-peak, Frequency: 0.01 μHz to 5 MHz
Power Amplifier	Amplitude: 0 to ± 20 V
Light Microscope	Zoom: 16×, 20×, 40×, 60×, 80×, 100×
Video camera	23.3 MP, sensor size ½.3 in, maximum video resolution 4K (3840×2160 pixel)
Video Processing Software	In-house algorithm implemented in MATLAB (2022b, MathWorks)
PC	Intel® Core i7-11370H, 32 GB RAM, NVIDIA® RTX™ 3050 Ti

The power supply instrumentation has been configured to generate a trapezoidal ramp signal in the range 0-20 V, and several videos of the DUT have been acquired considering a duration of least thirty periods of the supply signal. In particular, videos of the comb-drive at 40× magnification and videos of the CSFH and of the comb-drive's free end at 80× magnification have been acquired for evaluating the angular displacement. The acquired videos have been processed in MATLAB environment, and the comb-drive angular displacement has been measured by image tracking of many virtual markers positioned within predetermined regions of interest frame by frame.

B. Finite Element Analysis

Numerical simulations have been carried out using the commercial software COMSOL Multiphysics. In order to reduce computational costs, FEA simulations have been performed using the 2D model of the MG, to which was added an out-of-plane thickness of 40 μm. In particular, the 2D model was implemented from the CAD drawing used to create the aluminum hard mask of the fabrication process. To accurately replicate the electrostatic actuation of the comb-drive, the numerical model included the air surrounding the DUT as a free deforming domain. The mesh has been particularly optimized for the thinnest elements of the MG and in the air domain, thus obtaining about 71,000 triangular elements constituting the entire mesh. Non-linearities caused by large deflections have also been considered. The material utilized in the numerical simulations of the MG is Silicon <100>, which is also the material used in the manufacturing of the DUT. The material's Young's modulus is in accordance with [20].

III. UNCERTAINTY ANALYSIS

In order to discuss the outcomes of the study, an uncertainty analysis has been carried out, taking into

Table 3. Uncertainty sources in the experimental tests

Source of uncertainty	Value
Function generator amplitude	1% of $V_{peak\text{-}to\text{-}peak}$ + 2 mV
Power amplifier amplitude	2 mV
Optical system	1 µm
Video tracking algorithm	0.05°

account the main sources of error in the experimental analysis. Uncertainties have been expressed as standard deviations and the total uncertainty (σ_T) has been determined by combining Type A (σ_A) and Type B (σ_B) uncertainties as the root sum of squares as described in [21]. Type A uncertainties can be determined directly from the standard deviation of the obtained results, while Type B uncertainties have been computed using the error sources retrieved from the datasheets of the devices (Table 3). The optical system's uncertainty has been overall estimated to be 1 µm because of the lateral resolution, which is dependent on the incident light diffraction and wavelength, and the pixel resolution [22], as well as the uncertainty of the measurement procedure, which has been evaluated using a Monte Carlo Simulation (MCS) with 10^4 iterations. The total number of virtual markers inserted in the ROIs has been made to vary randomly, together with their relative coordinates, at each MCS iteration, which results in a variation of the x- and y-coordinates of the markers' centroid. As regards the uncertainty of the results obtained with the FEA, the geometric dimensions of the MG have been made to vary with an MCS with 10^4 iterations, considering the uncertainty caused by the DRIE process [8]. Finally, the uncertainty associated with the micro actuator's torque evaluation has been estimated by propagating the uncertainties of both the stiffness coefficient in (2) and the comb-drive's rotation [23].

IV. RESULTS AND DISCUSSION

Fig. 3 depicts the comb-drive displacement as

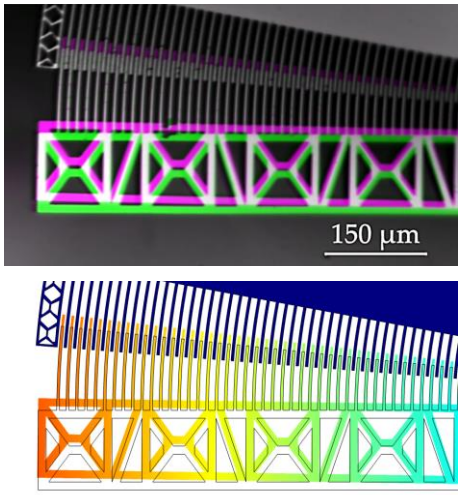

(a)

(b)

Fig. 3. Maximum displacement of the comb-drive evaluated by (a) experimental analysis and (b) FEA.

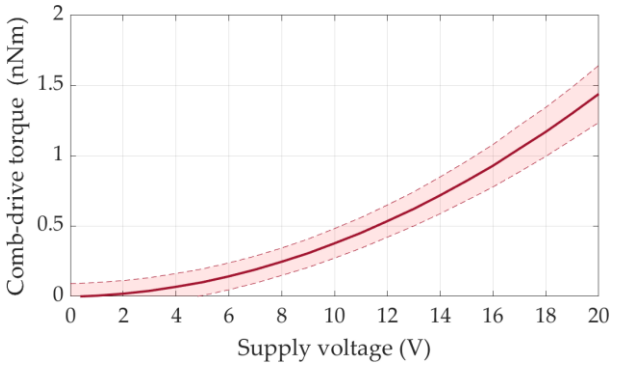

Fig. 4. Torque applied by the micro-actuator as a function of the supply voltage.

determined by means of both experimental and finite element analyses, applying to the MG a power supply in the range of 0-20 V peak-to-peak. According to the obtained results, the maximum displacement is 17.1 ± 1.1 µm, which corresponds to a rotation of 0.79° ± 0.05°. The curved beam stiffness coefficient has been evaluated at 0.10 ± 0.01 µNm/rad. This means that the comb-drive applies a torque of 1.4 ± 0.2 nNm in order to deform the CSFH of the collected angular displacement. Fig. 4 shows the evolution of the torque applied by the micro-actuator as a function of the supply voltage. In particular, torque is a function of the square of the supply voltage, which is consistent with the literature [10,24], both as trend and as order of magnitude.

V. CONCLUSIONS

The present study focused on a preliminary evaluation of the torque applied by the micro-actuator of a MG prototype equipped with a pair of CSFHs and electrostatic rotary comb-drives. Experimental and finite element analyses have been used in order to estimate the dynamic characteristics of the prototype. Videos of the DUT have been acquired using a trinocular optical microscope equipped with a video camera, which have been subsequently elaborated with an in-house algorithm implemented in MATLAB, and numerical simulations have been performed in COMSOL Multiphysics. Moreover, an uncertainty analysis has been carried out to assess the quality of the obtained results, which revealed that the micro-actuator under test is able to apply a maximum torque of 1.4 ± 0.2 nNm. In the near future, it will be important to improve the experimental setup as well as the numerical model used during the FEA and to carry out experimental tests to evaluate the torque applied by the micro-actuators when the MG performs a grasping and manipulation operation.

REFERENCES

[1] Z. Lyu, Q. Xu, "Recent design and development of piezoelectric-actuated compliant microgrippers: A review", Sensors and Actuators A: Physical, vol.331, November 2021, 113002.

[2] S. Gunasekaran, S. Periyagounder, S. Annamalai, A. Balaji, "Design and analysis of compliant micrograpper - A review," AIP Conference Proceedings, 2020, vol.2283, No.1.

[3] S. Yang, Q. Xu, "A review on actuation and sensing techniques for MEMS-based microgrippers", Journal of Micro-Bio Robotics, vol.13, No.1–4, October 2017, pp. 1–14.

[4] D. O. Otuya, Y. Verma, H. Farrokhi, L. Higgins, M. Rosenberg, C. Damman, et al., "Non-endoscopic biopsy techniques: a review", Expert Rev Gastroenterol Hepatol, vol.12, No.2, February 2018, pp. 109–117.

[5] K. R. Oldham, "Applications of MEMS technologies for minimally invasive medical procedures", in "MEMS for Biomedical Applications", Woodhead Publishing, 2012, pp. 269–290.

[6] T. Nishimura, Y. Fujihira, T. Watanabe, "Micrograpper-Embedded Fluid Fingertip-Enhancing Positioning and Holding Abilities for Versatile Grasping", J. Mechanisms Robotics, vol.9, No.6, October 2017, 061017.

[7] J. Zhang, O. Onaizah, K. Middleton, L. You, E. Diller, "Reliable Grasping of Three-Dimensional Untethered Mobile Magnetic Micrograpper for Autonomous Pick-and-Place", IEEE Robotics and Automation Letters, vol.2, No.2, April 2017, pp. 835–840.

[8] N. P. Belfiore, G. B. Broggiato, M. Verotti, R. Crescenzi, M. Balucani, A. Bagolini, et al., "Development of a MEMS technology CSFH based micrograpper," Proc. of 23rd International Conference on Robotics in Alpe-Adria-Danube Region (RAAD), 2014, pp. 1–8.

[9] N. P. Belfiore, G. B. Broggiato, M. Verotti, M. Balucani, R. Crescenzi, A. Bagolini, et al., "Simulation and construction of a mems CSFH based micrograpper", International Journal of Mechanics and Control, vol.16, No. 1, January 2015, pp. 21–30.

[10] F. Vurchio, P. Ursi, A. Buzzin, A. Veroli, A. Scorza, M. Verotti, et al., "Grasping and releasing agarose micro beads in water drops", Micromachines, vol.10, No.7, June 2019, pp. 1–15.

[11] F. Vurchio, F. Orsini, A. Scorza, S.A. Sciuto, "Functional characterization of MEMS Micrograpper prototype for biomedical application: Preliminary results," Proc. of 2019 IEEE International Symposium on Medical Measurements and Applications (MeMeA), 2019.

[12] R. Cecchi, M. Verotti, R. Capata, A. Dochshanov, G. B. Broggiato, R. Crescenzi, et al., "Development of micro-grippers for tissue and cell manipulation with direct morphological comparison", Micromachines, vol.6, No.11, November 2015, pp. 1710–1728.

[13] G. Bocchetta, G. Fiori, A. Scorza, N. P. Belfiore, S. A. Sciuto, "First results on the functional characterization of two rotary comb-drive actuated MEMS micrograpper with different geometry," Proc. of 25th IMEKO TC4 International Symposium and 23rd International Workshop on ADC and DAC Modelling and Testing, 2022, pp. 151–155.

[14] N. P. Belfiore, A. Bagolini, A. Rossi, G. Bocchetta, F. Vurchio, R. Crescenzi, et al., "Design, fabrication, testing and simulation of a rotary double comb drives actuated micrograpper", Micromachines, vol.12, No.10, October 2021, pp. 1–21.

[15] F. Vurchio, G. Fiori, A. Scorza, S. A. Sciuto, S. A. "A comparison among three different image analysis methods for the displacement measurement in a novel MEMS device," Proc. of. 24th IMEKO TC4 International Symposium and 22nd International Workshop on ADC and DAC Modelling and Testing, 2020, pp. 327–331.

[16] P. Ursi, A. Rossi, F. Botta, N. P. Belfiore, "Analytical Modeling of a New Compliant Microsystem for Atherectomy Operations", Micromachines, vol.13, No.7, July 2022, pp. 1094–1123.

[17] J. Liu, N. A. Abu Osman, M. Al Kouzbary, H. Al Kouzbary, N. A. Abd Razak, H. N. Shasmin, et al., "Stiffness estimation of planar spiral spring based on Gaussian process regression", Scientific Reports, vol.12, No.1, July 2022, pp. 1–15.

[18] A. Bagolini, S. Ronchin, P. Bellutti, M. Chistè, M. Verotti, N. P. Belfiore, "Fabrication of Novel MEMS Micrograpers by Deep Reactive Ion Etching with Metal Hard Mask", J. Microelectromechanical Syst., vol.26, No.4, May 2017, pp. 926–934.

[19] G. Bocchetta, G. Fiori, A. Scorza, S. A. Sciuto, "Image quality comparison of two different experimental setups for MEMS actuators functional evaluation: a preliminary study," Proc. of 25th IMEKO TC4 International Symposium and 23rd International Workshop on ADC and DAC Modelling and Testing, 2022, pp. 320–324.

[20] B. Bhushan, X. Li, "Micromechanical and tribological characterization of doped single-crystal silicon and polysilicon films for microelectromechanical systems devices", J. Mater. Res., vol.12, No.1, January 1997, pp. 54–63.

[21] J. R. Taylor, "An introduction to Error Analysis: The study of Uncertainties in Physical Measurements", 2nd edition, University Science Books, New York, USA, 1997.

[22] P.Prasad, "Introduction to Biophotonics", John Wiley and Sons, Inc, 2003.

[23] C. E. Papadopoulos, H. Yeung, "Uncertainty estimation and Monte Carlo simulation method", Flow Measurement and Instrumentation, vol.12, No.4, August 2001, pp. 291–298.

[24] C.-C. Tu, K. Fanchiang, C.-H. Liu, "1xN rotary vertical micromirror for optical switching applications," Proc. SPIE 5719, MOEMS and Miniaturized Systems V, 2005, pp. 14–22.